Available online at www.sciencedirect.com
ScienceDirect
Journal of Sound and Vibration 311 (2008) 1325–1339
JOURNAL OF SOUND AND VIBRATION
www.elsevier.com/locate/jsvi

Modeling of influencing parameters in active noise control on an enclosure wall

Marco Tarabini[a,*], Alain Roure[b]

[a]Dipartimento di Meccanica, Politecnico di Milano - Polo Regionale di Lecco, Via M. d'Oggiono 18/A, 23900 Lecco, Italy
[b]Laboratoire de Mécanique et d'Acoustique, Centre National de la Recherche Scientifique, 31, Chemin Joseph Aguier 13402, Marseille Cedex 20, France

Received 10 November 2006; received in revised form 2 October 2007; accepted 10 October 2007
Available online 26 November 2007

Abstract

This paper investigates, by means of a numerical model, the possibility of using an active noise barrier to virtually reduce the acoustic transparency of a partition wall inside an enclosure. The room is modeled with the image method as a rectangular enclosure with a stationary point source; the active barrier is set up by an array of loudspeakers and error microphones and is meant to minimize the squared sound pressure on a wall with the use of a decentralized control. Simulations investigate the effects of the enclosure characteristics and of the barrier geometric parameters on the sound pressure attenuation on the controlled partition, on the whole enclosure potential energy and on the diagonal control stability. Performances are analyzed in a frequency range of 25–300 Hz at discrete 25 Hz steps. Influencing parameters and their effects on the system performances are identified with a statistical inference procedure. Simulation results have shown that it is possible to averagely reduce the sound pressure on the controlled partition. In the investigated configuration, the surface attenuation and the diagonal control stability are mainly driven by the distance between the loudspeakers and the error microphones and by the loudspeakers directivity; minor effects are due to the distance between the error microphones and the wall, by the wall reflectivity and by the active barrier grid meshing. Room dimensions and source position have negligible effects. Experimental results point out the validity of the model and the efficiency of the barrier in the reduction of the wall acoustic transparency.

1. Backgrounds

Due to the increasing request for noiseless environments, active noise control [1] in enclosures is the focal point of many recent research studies [2–4]. There are basically two approaches to the active noise control (hereafter referred to as ANC) in enclosed spaces, that are the global and the local control [4]. The global control is meant to reduce the sound pressure at all points inside an enclosure [5,6] whilst local control is expected to create a quiet zone inside the room [7,8] without taking into account what happens outside the controlled volume. When the goal is the low-frequency noise attenuation in buildings, sometimes the structure-borne sound can be hardly reduced by means of an appropriate vibration isolation design [4,9];

*Corresponding author.
E-mail address: marco.tarabini@polimi.it (M. Tarabini).

0022-460X/$ - see front matter © 2007 Elsevier Ltd. All rights reserved.
doi:10.1016/j.jsv.2007.10.015

consequently, the low-frequency noise can be very annoying also in rooms adjacent to the one where the noise source is stored. Some investigations on the possibility of simultaneous noise and vibration control (in a very particular case, i.e. aircrafts cabin), have shown that difficulties may arise in terms of number of actuator required [10].

If the target is the reduction of noise irradiated towards a room contiguous to the one containing the sound source, it is reasonable to setup a local ANC by placing the error microphones and the secondary sources near the partition wall. The creation of a silent zone close to the division wall will probably lead to an attenuation of noise transmitted between the two rooms, with the great advantage of operating only in the room where the noise source is placed. For current purposes, a viable way seems to be the use of the active barrier technique [11–13] in order to control the acoustic energy (potential or kinetic) on the dividing wall. In an active noise barrier a loudspeaker array is used so as to create a quiet zone on a surface by generating destructive interference where the error microphone array is placed. Such technology has been used in open space areas in order to create destructive interference in limited volume portions, both for fixed [11] and moving [12,13] sources. Of particular interest is the use of a diagonal active barrier (hereafter DAB) as in Ref. [13]. In a DAB a decentralized feedforward algorithm is used, allowing to simplify the control system in N mono channel control units instead of a $N \times N$ global control system.

The use of a DAB at the vicinity of a dividing wall to reduce the noise transmission is of great interest if three main conditions are satisfied:

- the noise cancellation on the error microphones (placed close to the wall) leads to a significant mean attenuation on the wall surface and virtually rise the transmission loss of the partition;
- the reduction of acoustic energy on a wall does not significantly rise the acoustic energy of the whole enclosure;
- the geometric DAB configuration that allows a stable decentralized control does not lead to a noise reduction significantly different from the one of a global control.

To date, active noise barriers have never been used to reduce the acoustic transparency of a partition wall and consequently, in literature, there are no studies whose target is the optimization of a DAB in order to achieve these goals.

This paper has therefore three main objectives: the first is the investigation of the possibility of averagely reducing sound pressure on an enclosure wall by means of the decentralized ANC. The second target is the identification of the influencing parameters that affect the DAB performances. The last is the evaluation of the contribution of each parameter on pressure reduction and on the feedforward control stability. All these tasks are performed analyzing simulation results with the analysis of variance (ANOVA), which analyze data depending on the interaction of many different factors whose weight is to be determined [14].

Possibly influencing factors have been searched among the ones that describe the geometric configuration of the array and the ones that affect the acoustic behavior of the enclosure where the ANC is performed.

2. Acoustic model of the enclosure

The possibility of using an active barrier to reduce the acoustic transparency of a partition wall is investigated by simulating sound field in a noisy rectangular room with and without the ANC. The noise source is simulated as a point monopole placed in different positions of the room; the acoustic field that it generates is modeled with the virtual image sources technique, that identifies the images of the "real" source by a mirror effect on each enclosure boundary [15,16]. The image source technique has been chosen for the following reasons:

- the validity of the image source model for the determination of the point-to-point transfer function of the room across a wide frequency range has already been demonstrated [15];
- due to the important number of calculation to do, the model had to be relatively simple. For parallelepiped room, punctual sources and not too absorbent rigid walls, the image technique has been found to be well appropriated [15].

- the near field conditions (that are compulsory for the simulation of the behavior of secondary sources) and the time-domain response of the room are accurately modeled with a lower computational effort with respect, for example, to the modal analysis [15,17];
- aim of this paper is not the simulation of the acoustic field in the enclosure, but is the determination of the parameters that have an influence on the ANC performances. Thus, approximations introduced by the image source method are expected to be negligible.

A general conviction is that the geometric methods are not valid at low frequencies. This is actually true with the traditional image source approach, where the Sound Pressure Level is obtained by adding the contribution of each image assuming that sources are uncorrelated. In the adopted model, when computing the contribution of different sources, also the phase of the sound wave is considered. As pointed out in Ref. [17], the results obtained with this approach of the image source method are consistent with the ones of Boundary Element Method model also below 50 Hz. The comparison between the model prediction and preliminary experimental results (reported at the end of this paper) have shown the consistency of the adopted method as well.

Let us consider a monopole source of strength Q located inside an enclosure. In order to take into account the reflections given by the room boundaries, in correspondence of each wall, an image source with a strength rQ is considered, where r is the reflection coefficient of the surface [18]. Because of r definition, for each reflection on the wall, a fraction $(1-r^2)$ of the incident energy is absorbed. The propagation path of the reflected ray corresponds to the direction from the image source to the receiving point. Since all the six enclosure boundaries have to be considered, second and higher order image sources are generated, corresponding to rays that underwent multiple reflections.

The sound pressure produced by the monopole source located at S at a generic point M and at angular frequency ω is given by

$$P(M,\omega) = \mathrm{i}k\rho cQ \sum_{j=0}^{\text{n. images}} r^{o(j)} \frac{\mathrm{e}^{-\mathrm{i}kR_{MS_j}}}{4\pi R_{MS_j}}, \tag{1}$$

where j is the index of the image source, $o(j)$ is the order of reflections for the source j and R_{MS_j} is the distance between the observation point M and the image source S_j. $j=0$ correspond to the primary source and $o(0)=0$.

A uniform reflection coefficient (independent from the sound wave angle of incidence and from the frequency) has been used, with the advantages and implications pointed out by Allen and Berkley [15]. The number of image sources has been determined with a preliminary sensitivity analysis; the active barrier performances have been investigated as a function of the number of virtual sources on each room side. Results have shown that, in the investigated conditions, the use of more than five image sources for each side (totally 1330 virtual primary sources) leads to negligible changes (differences smaller than 0.3 dB) on simulation results. Thus, it has been chosen to use five virtual sources on each enclosure boundary. Obviously, the model takes into account also the image sources of each element of the loudspeaker array (i.e. secondary sources). Both the loudspeakers and the microphones that set up the active barrier are modeled as a point, thus neglecting scattering and diffraction effects. Another approximation is given by the infinite impedance of the model boundaries instead of their actual value: such approximation greatly simplifies the model but does not consider the coupling between the room vibration modes and the wall vibration modes.

The frequency range of simulations varies from 25 to 300 Hz with discrete steps of 25 Hz. Since the first natural frequency of the room is 34 or 50 Hz (depending on the adopted configuration), the maximum investigated frequency (300 Hz) is almost six times larger than the first room natural frequency. Conversely, the lowest investigated frequency (25 Hz) has been included to investigate the efficiency of the method at very low frequencies, where there is a growing interest in the acoustic behavior of enclosures [16]. In the practical problem for which simulations have been carried out, the largest part of noise is between 80 and 150 Hz, thus parameters of the ANC system has been optimized for these frequencies. Other frequencies have been included in the analysis so as to investigate the performances of active barriers in non-ideal conditions.

3. Analysis of variance and factorial design

The effects of the investigated influencing factors on the ANC efficiency have been studied with the ANOVA on a full factorial design. ANOVA allows determining whether some independent variables influence the dependent one (in our case the DAB performances). When ANOVA is performed on a factorial experimental design, independent variables are varied together so as to identify not only the effects of each single factor but also possible interaction among the independent variables [14]. Each independent variable can assume 2 values, that are conventionally called "High" and "Low". Consequently, if one wants to investigate K factors with their interactions, 2^K tests are required. The deduction about the influence of a factor (if it is significant or not) is obviously function of its "High" and "Low" values; anyway it is possible to extend the validity of conclusions to similar problems (i.e. small rooms with different dimensions, with non-uniform reflection coefficient, non-ideal loudspeakers, etc.). The result of the statistic inference is a probabilistic assessment about the influence of each parameter describing both the room and the ANC setup on the DAB efficiency. Bibliographical researches [11,13] and preliminary experiments outlined as possible influencing independent variables the ones listed in Table 1. Three factors are used to describe the enclosure where the DAB has to be setup and four parameters are used to describe the active barrier configuration.

Room Dimension have been included in the investigated parameters since DAB efficiency can depend on the room natural frequencies. The room dimensions have been selected so as to partially agree with the ones of the facility where the experimental campaign (not described in this paper) has been performed. It has been chosen to vary the room dimension by varying only the room depth, i.e. the wall where the active barrier is placed has always the same dimensions of $3 \times 2.6\,\mathrm{m}^2$. In this way, the room volume and natural frequencies can be modified independently from the active barrier arrangement. The room depth levels are set to 3.5 m (low) and 5 m (high). With such a configuration, the first natural frequencies of the room are approximately 50 and 35 Hz.

The influence of the primary source position has been investigated since the active barrier usually works better when the system can be placed close to the source [1]. Thus, two source positions (independent from the active barrier configuration and room dimensions) have been chosen. With reference to Fig. 1 the source position is characterized by the values h, k and d. Values h and k were fixed and, respectively, equal to 0.75 and 1.05 m since preliminary simulations pointed out their negligible effect on the DAB performances. The distance d can assume two values, that are 1.85 m (low) or 3.05 m (high). In the investigated frequency range, the source is reasonably far from the modal nodes.

The wall reflectivity is another factor that heavily influences the acoustic field inside the enclosure. The two levels of the reflection coefficient r are 0.55 (low) and 0.9 (high). The two values are representative of a considerably damped room and a heavily reflective one and thus allow simulating DAB performances in opposite conditions.

When taking into account the parameters describing the configuration of the DAB, preliminary explorative tests and simulations have shown that the distance between the loudspeakers and the error microphones (*dml* in Fig. 2) plays a key role both for the decentralized control stability and for the acoustic energy attenuation. The two levels of *dml* have been chosen to reduce the crosstalk effect between array elements and are 0.15 m (low) and 0.4 m (high).

Table 1
Independent variables and their levels

Factor	Name	Low (−1)	High (+1)
Room dimension	*A*	$3.5 \times 3 \times 2.6$	$5 \times 3 \times 2.6$
Source position	*B*	Near (1.85 m)	Far (3.05 m)
Distance LSP–MIC	*C*	0.15 m	0.4 m
Grid size	*D*	0.6 m	0.9 m
Wall reflectivity	*E*	0.55	0.9
Distance MERR–WALL	*F*	0.1 m	0.5 m
Loudspeaker directivity	*G*	Monopole	Dipole

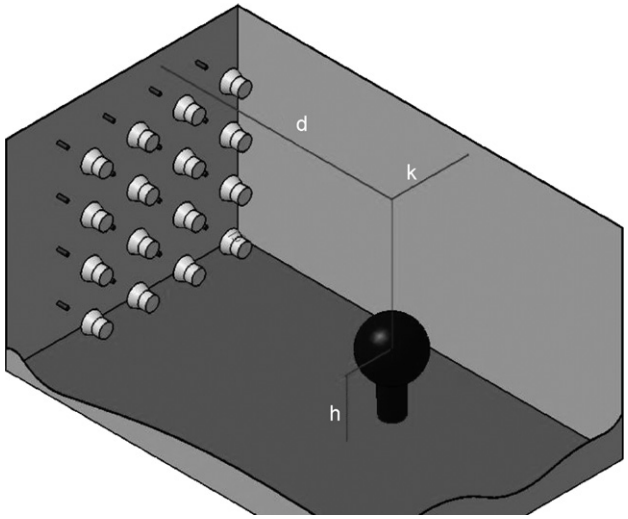

Fig. 1. Position of the primary noise source inside the enclosure: d is the distance from the partition to be controlled, h is the height above the floor and k is the distance from the lateral surface.

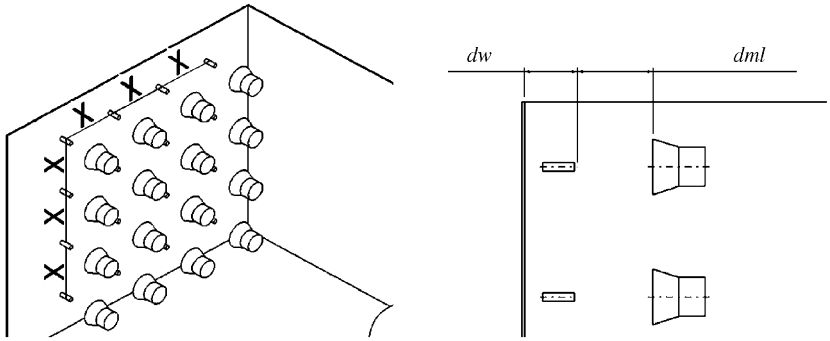

Fig. 2. Parameters used to describe the geometric configuration of the active barrier and its position with respect to the partition to be controlled. X is the distance between array elements; dw is the distance between the error microphones array and the partition wall and dml is the distance between the secondary source array and the error microphone array.

Another possibly influencing parameter is represented by the distance between the error microphone and the wall surface (dw of Fig. 2). Elliott et al. [19] observed that, with a traditional ANC system, a silent zone can be formed inside a diameter of about one-tenth of the acoustic wavelength around the error sensor in a fully diffused near sound field. Even if it can be expected a bigger quiet zone due to the proximity of the reflecting wall, we tested the influence of dw for two values (0.1 and 0.5 m).

The distance between two adjacent error microphones (in Fig. 2) is another parameter that may affect the active barrier performances. Literature studies [13] show that in free field conditions the maximum efficiency is reached when X is at most half of the wavelength of the acoustic radiation to be controlled. Since sound propagation in reverberant enclosures is much more complex than the free field one, it has been preferred to include this factor in the analysis. The two levels, that are 0.6 m (low) and 0.9 m (high), allow having active barriers with the same outer dimensions ($1.8 \times 1.8\,m^2$), respectively, made by 16 and 9 loudspeakers. According to the previously listed half-wavelength concept these two grid meshes should grant the same results up to approximately 180 Hz. This frequency is larger than the one of interest for the practical problem for which the active barrier has been designed.

The last factor to be investigated is the loudspeakers directivity. The control algorithm should be much more stable when using dipoles instead of monopoles since the crosstalk between adjacent elements is reduced by the dipole directional characteristics. Two different loudspeakers types (monopoles and

dipoles with a separating distance of 0.2 m) have been investigated. Dipole axis is perpendicular to the controlled partition.

3.1. Dependent variables

The dependent variables chosen to summarize the performance of the ANC system are the attenuation averaged on the partition to be controlled, the attenuation averaged on the whole enclosure volume and the lower eigenvalue of the control matrix. With the proposed image source model, the first two variables are evaluated at discrete points placed over a regular grid with a 0.2 m spacing. Simulations have shown that a reduction of such a distance does not meaningfully change the dependent variables.

The effect of the active control on each measurement point can be described with the ratio between the sound pressure without and with the ANC system expressed in dB. Such a ratio is calculated under the hypothesis of decentralized algorithm convergence consequently, if the algorithm is not stable (which will be taken into account by another dependent variable), the model will overestimate the actual ANC performances. The point attenuation (PA(f)) depends on the frequency and is defined for any point inside the room as

$$\mathrm{PA}(f) = 20\,\log\left|\frac{P_0(f)}{P(f)}\right|, \tag{2}$$

where $P_0(f)$ is the primary noise and $P(f)$ the noise after control.

The control is supposed to be perfect. That means that the strengths vector $\mathbf{Q}(f)$ of the secondary source is obtained in resolving the matricial equation:

$$\mathbf{Q}(f) = -\mathbf{H}(f)^{-1} \cdot \mathbf{P}_0^{\mathrm{err}}(f), \tag{3}$$

where $\mathbf{H}(f)$ is the transfer function matrix between all the array sources and all the array error microphones and $\mathbf{P}_0^{\mathrm{err}}(f)$ is the primary sound pressure vector on the array of error microphones. ANC effectiveness has been summarized with two parameters describing the control effects on the wall surface and on the whole enclosure volume.

The first dependent variable that is used to outline the effects of the DAB is the Area-Averaged Attenuation (hereafter AAA), that is basically the mean attenuation on all the points of the controlled partition surface. Points where AAA(f) has been evaluated are shown in Fig. 3:

$$\mathrm{AAA}(f) = 10\,\log\frac{\sum_{\mathrm{Surface}}\left|P_0(f)\right|^2}{\sum_{\mathrm{Surface}}\left|P(f)\right|^2}, \tag{4}$$

when AAA is positive, the active control system attenuates the global pressure level at a certain frequency; on the contrary, when AAA is negative the active control system amplifies the noise on the surface. In our model, AAA is calculated on 224 points that, as already outlined, are placed over a rectangular grid with a 0.2 m mesh. The second parameter used to check the active barrier performances is the volume-averaged attenuation (hereafter VAA) that is the attenuation on the whole enclosure volume

$$\mathrm{VAA}(f) = 10\,\log\frac{\sum_{\mathrm{Volume}}\left|P_0(f)\right|^2}{\sum_{\mathrm{Volume}}\left|P(f)\right|^2}. \tag{5}$$

A common issue in the ANC problems is that far from the error microphones it is possible to have negative PA values (i.e. the ANC rise the noise level instead of reducing it). Thus the VAA(f) allows quantifying magnitude of the disturbance introduced by the active barrier on the non-controlled areas. In our model the VAA is calculated on 4032 or 5824 points depending on the room volume (Fig. 3).

The last independent variable describes the possibility of having instability problems in the ANC algorithm. As mentioned in Ref. [20], the condition for a stable decentralized control at frequency f is that the real part of

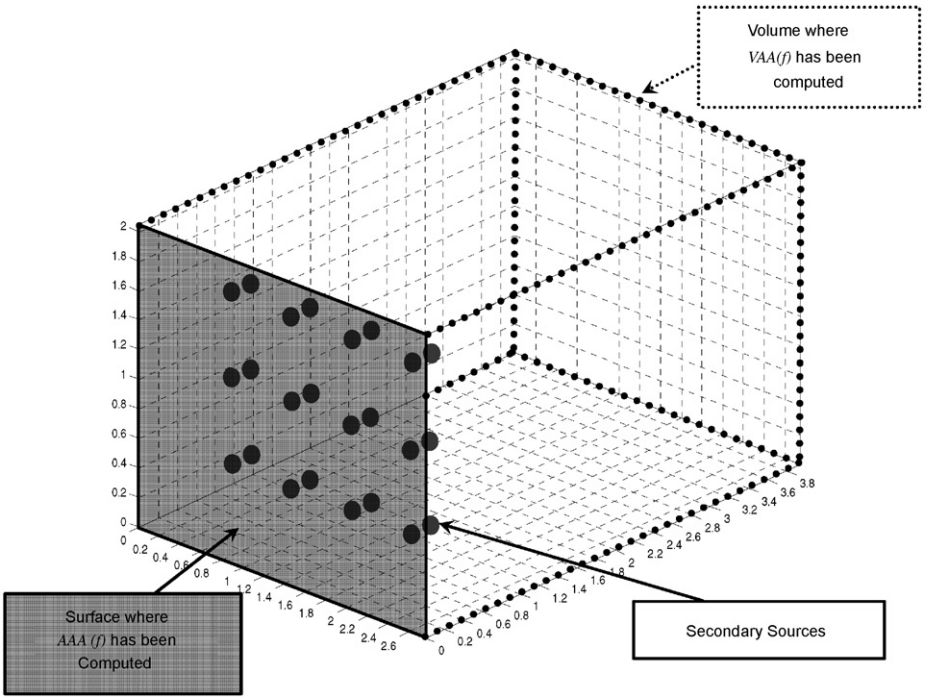

Fig. 3. Surface and volume where the dependent variables have been computed. The 12 pairs of circles symbolize the array of secondary sources (dipoles). Points of evaluation of AAA(f) and VAA(f) are placed over a regular grid (plotted only on the lateral surfaces) with spacing of 0.2 m.

the smallest eigenvalue of the matrix $\mathbf{G}(f) = \mathbf{D}^*(f) \cdot \mathbf{H}(f)$ is positive. $\mathbf{D}^*(f)$ is the conjugate complex of the diagonal of $\mathbf{H}(f)$. The system stability is checked with the least eigenvalue of the control matrix $\mathbf{G}$, LEG(f).

$$\mathrm{LEG}(f) = \min\{\mathrm{eig}(\mathbf{G}(f))\}. \tag{6}$$

The result of the ANOVA is a regression model that can be used to predict the dependent variable with a specific combination of the independent ones. Since the model can be helpful in order to roughly estimate the effects of configuration changing, it has been chosen to include the regression coefficient of meaningful factors among the results in the Appendix. The dependent variable model is

$$\xi = \beta_0 + \beta_1 x_1 + \beta_2 x_2 + \beta_3 x_3 + \beta_{12} x_1 x_2 + \beta_{123} x_1 x_2 x_3 + \cdots + \varepsilon, \tag{7}$$

where ξ is the dependent variable (AAA(f), VAA(f) or LEG(f)) and x_i are the independent variables expressed in coded units (the variables can assume values of -1 or $+1$, respectively, for low and high level). β_0 is the global tests average, β_i, $\beta_{i,j}$ and $\beta_{i,j,k}$ are used to describe the effect of the independent variables and their interactions. ε is the residual, namely the difference between the actual data behavior and the model prevision. The interactions between two or more variables are modeled by introducing a cross-product term in the multivariate regression [14].

Although simulation results were available with 16-bits precision, the hypothesis testing have been performed on AAA(f), VAA(f) and LEG(f) with three significant digits.

The ANOVA essentially tests the hypothesis that the variance introduced by the investigated factor is important with respect to the variance of the residuals. When performing the ANOVA on a full factorial design, if we consider the higher order available model, the residuals are given by the variance introduced by test repetitions. Since our results are obtained by simulations, each repetition leads to the same result and the ANOVA would be meaningless. Thus instead of using a model that takes into account interactions up to the seventh order, it has been chosen to exclude from the model interactions of third and higher order. Such simplification has been undertaken so as to have a model whose ''physical'' meaning can be easily understood. The exclusion of possibly meaningful interactions increases the dispersion of the residuals. Since the standard

Table 2
Standard deviation of errors and adjusted R^2 as a function of frequency

	Frequency (Hz)											
	25	50	75	100	125	150	175	200	225	250	275	300
SD error AAA(f) (dB)	2.9	2.9	2.4	3.0	2.1	1.5	1.8	2.4	2.6	1.4	2.8	2.0
SD error VAA(f) (dB)	0.8	1.6	1.2	1.8	0.9	1.1	1.2	1.0	1.4	0.9	1.4	0.9
SD error LEG(f) (thousands)	0.2	4.0	8.5	8.7	21.0	14.6	30.5	49.7	41.7	55.6	77.4	114.0
R^2_{adj} (%) AAA(f)	89.9	90.8	92.2	80.7	84.3	85	70.3	66.4	51.7	76	54.9	57.7
R^2_{adj} (%) VAA(f)	92.1	86	86.5	65.6	84.9	80.5	64.8	74.5	61.5	73.8	51.2	67.7
R^2_{adj} (%) LEG(f)	99.9	99.6	98.5	99.5	98.7	99.62	99.3	98.7	99.5	99.5	99.3	98.9

deviation of residuals represents the threshold for the significance of the dependent variables (a factor is meaningful if the variance that it introduces is larger than the variance of residuals), neglecting interactions leads to increasing the limit at which a factor is considered "important". The use of the simplified second-order model leads to the standard deviations of residuals listed in Table 2. In practice, ANOVA has been used like a multiple hypotheses testing with the threshold levels of Table 2. Since the residuals of AAA(f) are in the range between 1 and 3 dB, factors are judged as important if their effects are statistically larger than values of Table 2 (i.e. 3 dB). These values are representative of the differences that can be expected between the simulation results and the actual tests results. Table 2 also shows the coefficients of multiple determination R^2_{adj}, that indicate the capability of the model in describing the actual data behavior [14].

4. Simulation results

The first step of the ANOVA is the analysis of residuals, whose target is to outline information about model inadequacies [14]. The hypothesis of normality of residuals for the three independent variables is not always satisfied and consequently the second-order model does not always accurately describe simulation results. More detailed analyses have shown that this happens at frequencies very close to room modes. Since aim of this paper is the analysis of influencing parameters and not the study of an accurate regression model, the non-normality of residuals is not a critical issue.

ANOVA results are summarized in terms of P-values and coefficients of the regression model. Hypothesis H_0 (i.e. the factor is not relevant with the respect of the thresholds of Table 2) is rejected if P-value is lower than α, the type I error risk, that was set to 5%.

4.1. Area-averaged attenuation

Independent variables effects on AAA(f) are shown in Fig. 4, that points out two meaningful issues. The first is that the mean attenuation ranges between the 13 dB at 25 Hz and 4 dB at 150 Hz; consequently sound pressure on the partition is averagely reduced by the active barrier of these quantities. The second is that, since the line tilt is proportional to the influence of each variable, most influencing factors are the distance between loudspeakers and error microphones and the loudspeaker directivity.

Results are also summarized in Table 3, that shows the P-values for the AAA(f) for frequencies up to 300 Hz and the model coefficients up to 150 Hz. Coefficients for larger frequencies are not included since R^2_{adj} values (Table 1) point out an insufficient second-order model accuracy. Since the threshold levels for the AAA(f) ranges between 1.4 and 3 dB, depending on the frequency, a factor is considered as influencing if its variation between high and low level implies a difference in the area attenuation that is statistically greater than these levels. When model coefficients are positive, the AAA(f) is larger when the factor has the "high" value and vice versa; the numeric value of the coefficient quantifies the effect of the variable. A brief discussion of the effects that the dependent variables have on the AAA is hereafter presented.

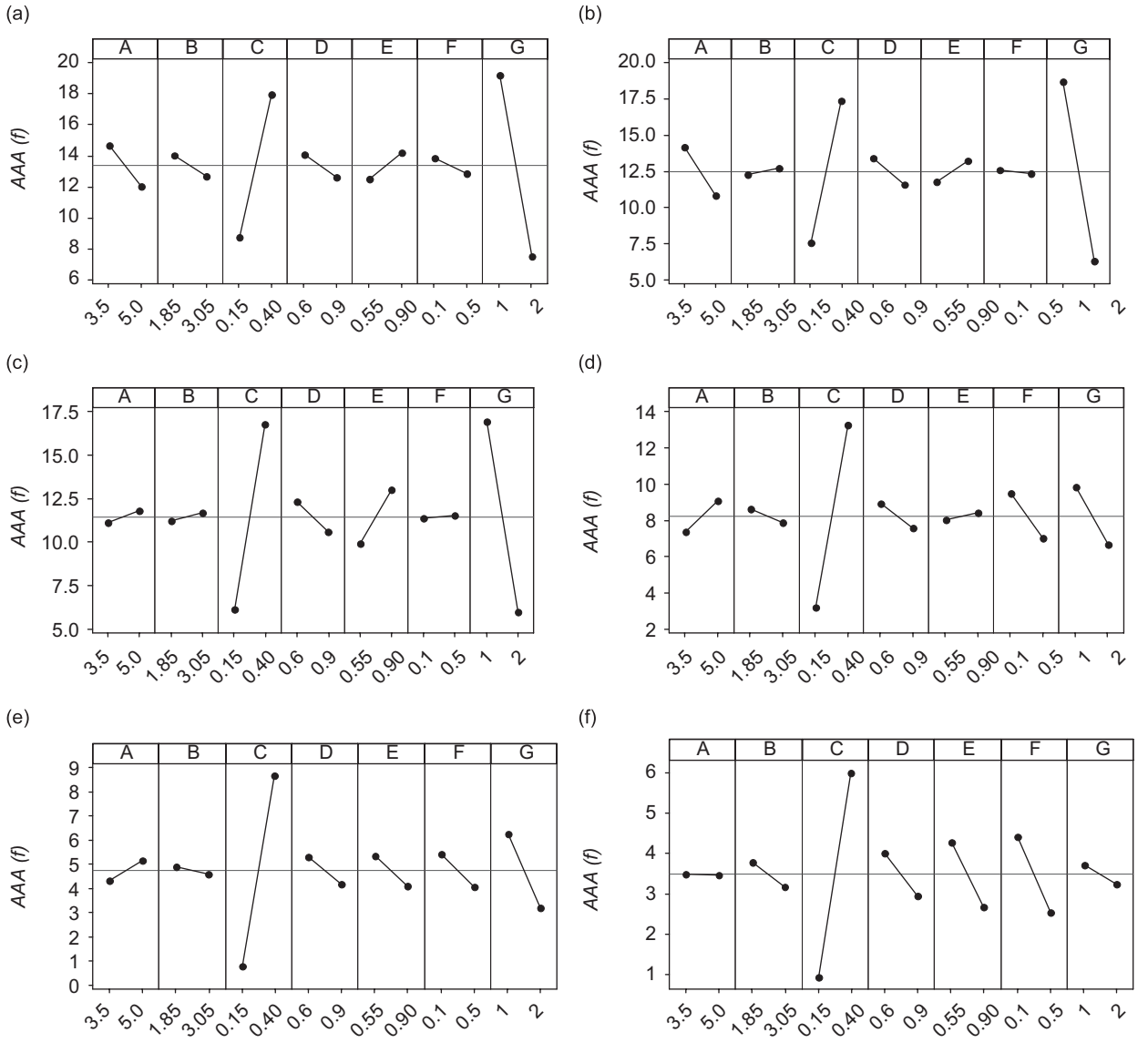

Fig. 4. Main effect plots on the Area-Averaged Attenuation as a function of frequency: (a) 25 Hz, (b) 50 Hz, (c) 75 Hz, (d) 100 Hz, (e) 125 Hz, and (f) 150 Hz. *x*-axis symbolizes factor levels. Line tilt of each of the seven lines is proportional to the factor effect. Horizontal line represents the average of all the 128 simulations.

Room Dimension has a limited influence on AAA(*f*): in the frequency range for which the DAB has been designed the *P*-value is larger than the meaningfulness threshold (5%) only for six frequencies over the 12 investigated. At some frequencies the attenuation given by the ANC system is larger when the room is small, while some others vice versa.

In the investigated configurations *P*-values show that the Source Position does not affect the ANC performances. The analysis of main effects shows that for some frequencies better results can be obtained with the source close to the active barrier and in some other with the source far from the barrier, but the effect of this parameter seems to be limited.

Performances of the DAB are slightly improved in presence of highly reverberant surfaces. Such a result is mainly due to the fact that with the same source strength, sound pressure level in a reverberant room is larger

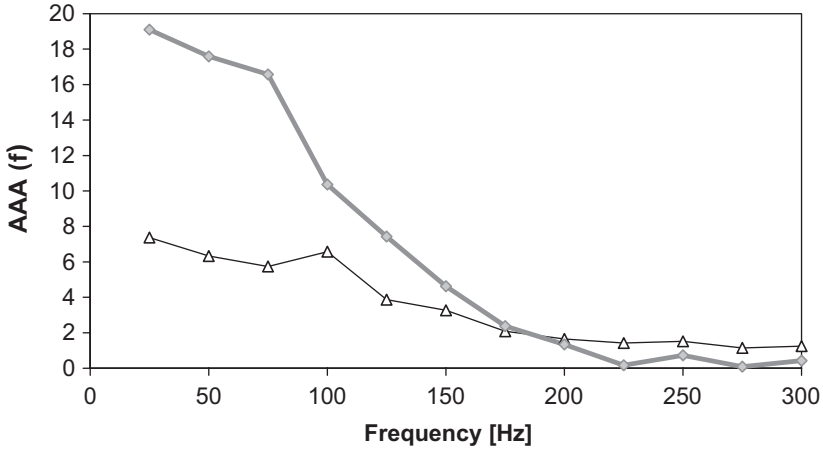

Fig. 5. Effect of loudspeaker directivity: family mean of AAA(f) as a function of frequency: (—△—) dipole source, and (— ◆—) monopole source.

than the one in a heavily damped enclosure. Anyway, despite the large difference between the two levels (reflection coefficients of 0.9 and 0.55) the P-value is not systematically larger than α, thus it seems reasonable to obtain good ANC performances both with absorbing and reverberant conditions.

Among parameters describing the configuration of the active barrier, the distance between the loudspeakers and the error microphones systematically influences the ANC performances. The analysis of main effects demonstrates that the active barrier works much better when the distance between microphones and loudspeaker is large, independently from the frequency.

The distance between the error microphone array and the wall surface has a partial influence on the AAA(f). P-value is smaller than α only for frequencies between 100 and 200 Hz where better performances are achieved with the error microphone close to the surface. Globally, the coefficients of the regression model (at most 1.1 dB) highlight the reduced effect of this parameter.

Despite in free field conditions, when matching the half-wavelength criterion, the ANC system performances does not considerably depend on grid meshing, ANOVA results outline that inside enclosures this factor systematically influences AAA(f). The analysis of main effects shows that a more dense mesh (0.6 m) allows reductions that are larger than the ones of a sparse configuration (0.9 m).

The loudspeakers directivity influences the AAA(f) for almost all frequencies: at low frequencies better performances are granted by monopoles, while at high frequencies dipoles allows larger noise attenuations. In the frequency range the DAB has been designed for, better performances are achieved with monopole sources, while above 150 Hz dipoles grants larger attenuations, as clearly shown in Fig. 5. Since the dipole directional characteristics are determined by the distance between the two monopole sources (0.2 m in this paper), the frequency for which dipoles acts better than monopoles describes only the investigated configuration.

In the frequency range of interest, the second-order interactions are almost negligible, since their effect is not systematic and depends on the frequency. Slight cross-effects exist at frequencies below 100 Hz between room dimensions and wall reflectivity and room dimensions and loudspeaker directivity. A more sensible interaction seems to exist between room dimension and wall reflectivity. At frequencies larger than 200 Hz an interaction exists between the distance loudspeaker-error microphones and the grid size.

4.2. Global enclosure energy

When an ANC system is used inside an enclosure, it is desirable that a reduction of noise on the controlled wall surface does not lead to heavy amplifications on the non-controlled areas. The VAA(f) parameter can be

therefore intended as an index of the disturbance introduced by the active barrier in the enclosure. The VAA(f) values range between 0.5 and −10 dB. This indicates that the ANC usually amplifies the energy content of the enclosure; the worst value of VAA(f) denotes a noticeable energy amplification, but is obtained with a configuration that has no practical interest since it does not allow noticeable AAA(f) values. Deeper investigations on VAA(f) have shown that the amplification is very large in the proximity of the loudspeaker array, but if is evaluated on the other enclosure walls is at most 4 dB on the lateral surfaces and 2 dB on the surface opposite to the one with the active barrier. In some applications, these values can be tolerated (especially if compared with the reductions achieved on the controlled wall); if the amplification on the other enclosure boundaries cannot be accepted, it is possible to optimize the ANC configuration in order to minimize this kind of disturbance.

Under this perspective the independent variables that systematically affect the VAA(f) are the distance between the loudspeakers and the error microphone and the loudspeakers directivity. The best performances in terms of global volume attenuations are achieved with monopole loudspeakers and with error microphones close to secondary sources. At low frequencies (below 100 Hz) VAA(f) partially depends on the source position and the wall reflectivity. The only systematic second-order effect is between the loudspeaker directivity and the distance between loudspeakers and the error microphones. Such an interaction points out that the combination of dipole loudspeakers and large X distance largely increases the global enclosure energy. In opposition to what previously seen for AAA(f), the grid spacing does not generally affect system performance in terms of total potential energy, i.e. the enclosure energy does not depend on the number of secondary sources.

4.3. Control stability

Among the investigated independent variables, four of them have a systematic influence on the **G** matrix eigenvalues and consequently on the control stability. Table 4 shows P-values and regression coefficients for those factors that the ANOVA have shown to be meaningful (with thresholds that varies from approximately 1 to 114 thousands). For each tested frequency, the control stability depends on the distance between loudspeakers and error microphones, on the wall reflectivity, on the distance between the error microphones and the wall surface and on the loudspeaker directivity. Furthermore, systematic second-order effects exist between:

- distance between loudspeakers and error microphones and wall reflectivity;
- distance between loudspeakers and error microphones and distance between error microphones and the wall;
- distance between loudspeakers and error microphones and loudspeaker directivity;
- distance between error microphones and the wall and loudspeaker directivity.

The behavior of LEG(f) is mainly driven by the distance between loudspeakers and error microphones, by the loudspeakers directivity and the interaction between these two factors. The feedforward algorithm is much more stable with dipole loudspeakers placed close to the error microphones. Additionally, the control is easier in highly damped rooms and whether the DAB is near to the controlled surface; the influence of other factors is considerably less important. Deeper investigations, performed with frequency steps of 2 Hz instead of 25 Hz, have shown that the instability problem mainly arises in correspondence of the room natural frequencies in slightly damped enclosures.

In the tested conditions, the stability of the control is not heavily influenced by the grid mesh, although generally in free field conditions the decentralized control algorithm is more stable with larger separating distances X. The coefficients of the regression model point out that the effect on the matrix eigenvalues is much smaller than the effects of the previously mentioned parameters. P-values are generally smaller than 5%, but are rarely lower than 1% (that is a more selective threshold). An ANOVA performed on a reduced number of variables with three levels for both grid size and distance between error microphones and loudspeakers have shown that the control stability is systematically influenced by an interaction between these two variables.

Consequently the instability arises when the distance between error microphones and loudspeaker is large compared with the grid size, as a function of frequency.

The recurrent second-order interactions outline that an optimization of the system stability can be achieved only by a rigorous study of a factorial design, so as to include in the analysis the ''cross effects'' among the independent variables.

5. Discussion

Results of simulations show that it is possible to averagely reduce the sound pressure level on a partition by means of the decentralized ANC. The averaged attenuation on the controlled surface AAA(f), the disturbance on the non-controlled volume VAA(f) and the feedforward control LEG(f) stability are mainly driven by the loudspeaker directivity and by the distance between loudspeakers and the error microphones. Generally those factors that theoretically allow larger AAA(f) lower the eigenvalues of the control matrix. The combinations that grant a good trade-off between DAB performances and control stability are given by monopole loudspeakers placed close to error microphones (in this paper the ''low'' separating distance was 0.15 m) or by dipole loudspeakers far (0.4 m) from the error sensors. The use of large separating distances between microphones and secondary sources theoretically increases the system performances but easily leads to negative eigenvalues of the control matrix. Setups with small separating distances allow stable control algorithms and, in practice, allow the use of higher convergence coefficients that may lead to larger attenuations. Therefore, the optimization for both monopole and dipole secondary sources consists in finding a good trade-off between performances and stability. In order to fully optimize the active barrier performances it is possible to leverage on those factors which have an influence on the control stability and not on surface noise attenuation and vice versa. Under this perspective ANOVA results have shown that, in the tested configuration, the **G** matrix eigenvalues moderately depend on the distance between the grid elements. Conversely, a more dense grid allows larger noise reductions and thus it is desirable to have more than two elements in a wavelength of the acoustic radiation to be controlled. If the distance between the error microphones and the wall surface is smaller than one-seventh of the acoustic wavelength, it has negligible effects on the surface noise attenuation. Since small distances grant and more positive matrix eigenvalues, it is desirable to place the control microphones as close as possible to the controlled surface. Simulations results have also outlined that system performances and stability are nearly independent from the enclosure dimensions and on the source position. The only enclosure-related variable that, in tested conditions, drives the system stability is the wall reflectivity, since control is easier in highly damped rooms (i.e. condition are close to the free field ones). The disturbance that the DAB introduces in the non-controlled part of the enclosure could be considered negligible in most applications (typical values are in the range of 2–4 dB). If an optimization in this direction is required, the use of monopole sources close to the error microphones has to be preferred. Although these conclusions depend on the numerical values of the independent variables, it is realistic to extend their validity to similar conditions.

In order to validate the results of simulations, preliminary experimental tests have been carried out in a small room with two surfaces covered with acoustically absorbent material and with the primary source placed at approximately 2 m from the active barrier sending a broadband noise (50–300 Hz). The DAB was setup with dipole sources placed at 0.5 m from the error microphones and with a grid mesh of 0.6 m. The decentralized control algorithm was a classical time-domain FXLMS algorithm. Model validity has been checked with the comparison of the AAA computed with the image source model (with model parameters describing the actual experimental setup) and the pressure reduction due to the DAB measured with eight microphones placed on the controlled surface (as far as possible from the error transducers). The comparison (Fig. 6) shows that experimental results and simulations have a similar behavior (differences lower than 3.5 dB) except at 80 Hz; the difference in the low-frequency region can be endorsed to the secondary sources used in our tests, that have a limited efficiency below 100 Hz and by causality problems due to the filtered white noise used in experiments. The most interesting result of the comparison is anyway that the DAB can be used to reduce sound pressure on the controlled surface and that such a reduction, at some frequencies is

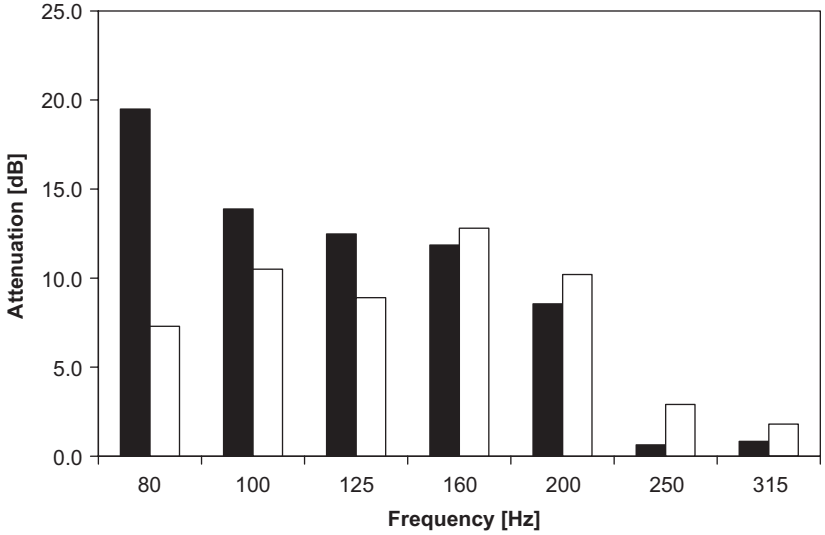

Fig. 6. Comparison between attenuation measured in preliminary tests (white) and results of simulations performed with the proposed image source model (black).

larger than 10 dB. Since similar pressure reductions have been measured also on the other side of the partition (i.e. in an adjacent room) it is evident that the DAB can be used to virtually reduce the acoustic transparency of a wall.

6. Conclusions

In this paper, the possibility of reducing sound pressure on an enclosure wall by means of an DAB has been investigated and discussed. The effects of variables that describe the enclosure and the active barrier configuration on the DAB performances have been investigated with simulations carried out with the image source method and analyzed with the ANOVA technique. Due to the practical problem for which the simulations have been done, the analyses have been carried out in a range of 25–300 Hz with steps of 25 Hz. Room dimensions have been chosen on the basis of the facility where the future experimental campaign will be carried out. Simulation results have pointed out that the DAB performances, in the investigated conditions, are driven by the loudspeaker directivity and by the distance between secondary sources and error microphones. As a result, combinations that allow a good compromise between theoretical attenuation and control stability are given by monopoles placed close to error microphones or by dipoles far from the error transducers. The effects of the distance between the error microphones and the wall, of the wall reflectivity and of the active barrier grid meshing are less important, as pointed out by the coefficient of the regression model listed in the Appendix. The influence of room dimensions and source position, with the adopted values of the independent variables seems to be negligible. The disturbance induced by the active barrier in the non-controlled areas is generally lower when using monopole loudspeakers placed close to the error sensors. Preliminary experimental tests have shown both the consistency of the proposed image source model and the possibility of reducing to more than 10 dB the sound pressure level on an enclosure wall. A similar noise reduction was also measured on the other side of the partition, consequently the DAB can be used in order to virtually reduce the acoustic transparency of dividing walls. The next step of the research will be the experimental investigation of the method performances on the basis of the results described in this paper.

Appendix

The numerical results of the ANOVA are hereafter presented in Tables 3 and 4.

Table 3
P-values and linear model coefficients of ANOVA on AAA(*f*)

	P-values—frequencies (Hz)												Model coefficient—frequencies (Hz)					
	25	50	75	100	125	150	175	200	225	250	275	300	25	50	75	100	125	150
k	**0.00**	**0.00**	**0.00**	**0.00**	**0.00**	**0.00**	**0.00**	**0.00**	**0.00**	**0.00**	**0.00**	**0.00**	13.2	12.0	11.2	8.5	5.6	3.9
A	**0.00**	**0.00**	0.06	0.03	0.48	0.36	0.01	0.02	0.52	**0.00**	0.43	0.33	−1.5	−2.2	0.4	0.5	0.1	−0.1
C	**0.00**	**0.00**	**0.00**	**0.00**	**0.00**	**0.00**	**0.00**	**0.00**	**0.00**	**0.00**	**0.00**	**0.00**	4.5	4.6	4.8	4.7	3.6	2.8
D	**0.00**	**0.00**	**0.00**	**0.01**	**0.00**	**0.00**	**0.00**	**0.00**	**0.00**	**0.00**	**0.00**	**0.00**	−0.8	−1.0	−0.9	−0.7	−0.6	−0.6
E	**0.00**	0.19	**0.00**	0.02	**0.01**	0.04	**0.00**	0.64	0.27	**0.00**	0.01	0.31	0.8	0.3	1.4	0.6	0.5	−0.2
F	0.09	0.65	0.91	**0.00**	**0.00**	**0.00**	**0.00**	0.01	0.78	0.68	0.70	**0.00**	−0.4	−0.1	0.0	−1.1	−0.9	−0.9
G	**0.00**	**0.00**	**0.00**	**0.00**	**0.00**	**0.00**	0.31	0.17	**0.00**	**0.00**	**0.00**	**0.00**	−5.9	−5.6	−5.4	−1.9	−1.8	−0.7
*A*B*	0.57	**0.00**	0.38	0.85	0.41	0.10	0.59	0.86	0.85	**0.00**	0.67	0.65	−0.1	−1.3	0.2	0.0	−0.1	0.2
*A*E*	**0.00**	**0.00**	0.64	**0.00**	0.80	0.10	0.03	0.54	0.18	0.02	0.01	0.24	−1.7	−0.9	−0.1	0.8	0.0	−0.2
*A*G*	**0.01**	**0.00**	**0.00**	0.02	0.17	0.50	**0.00**	0.68	0.98	0.60	0.16	0.16	0.7	1.5	−1.1	−0.6	0.2	0.1
*B*E*	0.33	0.09	**0.00**	0.93	0.10	0.11	0.62	0.73	0.94	0.19	0.59	0.30	−0.2	0.4	0.7	0.0	0.3	0.2
*C*D*	0.87	0.93	0.42	0.99	0.59	0.86	**0.00**	**0.00**	**0.00**	**0.00**	**0.00**	**0.00**	0.0	0.0	0.2	0.0	0.1	0.0
*C*E*	0.06	0.03	0.21	0.76	0.62	0.59	**0.00**	0.70	0.03	0.02	0.04	0.13	−0.5	−0.5	−0.2	0.1	−0.1	−0.1
*C*G*	**0.00**	0.07	0.69	0.11	0.20	**0.01**	0.21	0.02	0.98	0.08	0.17	0.03	1.1	0.4	−0.1	0.4	−0.2	−0.3
*D*E*	0.56	0.70	0.68	0.40	0.83	0.27	0.07	0.90	0.22	**0.00**	0.27	0.69	0.1	0.1	0.1	0.2	0.0	0.1
*D*G*	0.72	0.51	0.16	0.91	0.16	0.01	**0.00**	**0.00**	0.01	0.15	0.23	0.37	−0.1	0.1	0.3	0.0	0.2	0.3
*E*F*	0.05	0.18	0.24	0.02	**0.00**	**0.00**	0.96	0.05	0.85	**0.00**	0.02	0.44	−0.5	−0.3	−0.2	−0.6	−0.6	−0.5
*F*G*	**0.00**	0.14	0.47	**0.00**	**0.00**	0.04	0.09	0.99	0.57	0.29	0.05	0.14	0.7	0.3	0.1	0.9	0.8	0.2

P-values are evidenced with a bold number when smaller than 1%.

Table 4
P-values and linear model coefficients (expressed in thousands) of meaningful parameters of ANOVA for LEG(*f*)

	P-values—frequency (Hz)												Model coefficient (thousands)—frequencies (Hz)					
	25	50	75	100	125	150	175	200	225	250	275	300	25	50	75	100	125	150
k	**0.00**	**0.00**	**0.00**	**0.00**	**0.00**	**0.00**	**0.00**	**0.00**	**0.00**	**0.00**	**0.00**	**0.00**	4.4	14.7	32.1	63.8	92.5	146.5
A	0.06	**0.00**	0.04	0.40	0.27	0.10	0.15	0.93	0.62	0.85	0.01	0.21	0.0	−2.8	−1.6	−0.6	2.1	2.1
C	**0.00**	**0.00**	**0.00**	**0.00**	**0.00**	**0.00**	**0.00**	**0.00**	**0.00**	**0.00**	**0.00**	**0.00**	−4.2	−15.6	−33.3	−63.6	−92.3	−146.1
D	**0.00**	0.01	0.01	0.04	0.20	0.03	**0.00**	0.05	**0.00**	**0.00**	**0.00**	**0.00**	0.1	0.9	1.9	1.6	2.4	2.9
E	**0.00**	**0.00**	**0.00**	**0.00**	**0.00**	**0.00**	**0.00**	**0.00**	**0.00**	**0.00**	**0.00**	**0.00**	0.1	−1.9	−5.6	−6.3	−14.8	−8.0
F	**0.00**	**0.00**	**0.00**	**0.00**	**0.00**	**0.00**	**0.00**	**0.00**	**0.00**	0.81	**0.00**	0.98	−0.4	−1.4	−3.9	−6.9	−11.1	−17.7
G	**0.00**	**0.00**	**0.00**	**0.00**	**0.00**	**0.00**	**0.00**	**0.00**	**0.00**	**0.00**	**0.00**	**0.00**	3.2	15.6	34.3	58.6	88.5	133.9
*A*C*	0.28	**0.00**	0.14	0.56	0.34	0.50	0.15	0.89	0.53	0.56	0.02	0.33	0.0	1.4	1.1	0.4	−1.8	−0.9
*A*E*	0.74	**0.00**	**0.00**	0.49	0.44	**0.00**	0.91	0.80	0.84	0.02	0.66	0.38	0.0	−2.3	−2.4	−0.5	1.5	6.4
*A*G*	**0.00**	**0.00**	0.04	0.06	0.37	0.48	0.28	0.05	0.61	0.13	0.02	0.05	−0.1	2.7	−1.6	1.5	1.7	0.9
*C*D*	**0.00**	0.14	0.07	0.10	0.34	0.09	0.12	0.17	**0.00**	**0.00**	0.05	**0.00**	−0.1	−0.5	−1.4	−1.3	−1.8	−2.2
*C*E*	**0.00**	0.08	**0.00**	**0.00**	**0.00**	**0.00**	**0.00**	**0.00**	**0.00**	**0.00**	0.07	**0.00**	−0.1	0.6	3.3	4.6	11.7	4.4
*C*F*	**0.00**	**0.00**	**0.00**	**0.00**	**0.00**	**0.00**	**0.00**	**0.00**	**0.00**	0.03	**0.00**	0.03	0.3	1.5	4.0	6.6	11.5	15.0
*C*G*	**0.00**	**0.00**	**0.00**	**0.00**	**0.00**	**0.00**	**0.00**	**0.00**	**0.00**	**0.00**	**0.00**	**0.00**	−3.2	−14.3	−32.6	−56.8	−88.3	−128.6
*E*F*	**0.00**	0.86	0.31	0.29	0.60	0.17	0.26	0.84	0.12	**0.00**	0.17	0.26	−0.1	−0.1	−0.8	−0.8	−1.0	−1.8
*E*G*	0.60	**0.00**	**0.00**	**0.00**	0.35	**0.01**	0.24	0.03	0.18	0.02	0.94	0.35	0.0	2.4	4.1	5.3	1.8	3.7
*F*G*	**0.00**	0.06	**0.00**	**0.00**	**0.00**	**0.00**	**0.00**	**0.00**	**0.00**	0.01	**0.00**	0.02	−0.1	−0.7	−3.2	−3.5	−13.7	−7.3

P-values are evidenced with a bold number when smaller than 1%.

References

[1] S.J. Elliott, P.A. Nelson, *Active Control of Sound*, Academic Press Limited, London, 1992.
[2] Y.Y. Li, L. Cheng, Active noise control of a mechanically linked double panel system coupled with an acoustic enclosure, *Journal of Sound and Vibration* 297 (3–5) (2006) 1068–1074.

[3] M. Al-Bassyiouni, B. Balachandran, Control of enclosed sound fields using zero spillover schemes, *Journal of Sound and Vibration* 292 (3–5) (2006) 645–660.
[4] S.K. Lau, S.K. Tang, Sound fields in a slightly damped rectangular enclosure under active control, *Journal of Sound and Vibration* 238 (4) (2000) 637–660.
[5] S.D. Sommerfeldt, J.W. Parkins, Y.C. Park, Global active noise control in rectangular enclosures, *Proceedings of the ACTIVE '95*, Newport Beach, CA, 1995, pp. 477–488.
[6] P.A. Nelson, A.R.D. Curtis, S.J. Elliott, A.J. Bullmore, The active minimization of harmonic enclosed sound field. Part I: theory. *Journal of Sound and Vibration* 117 (1987) 1–13.
[7] P. Joseph, S.J. Elliott, P.A. Nelson, Near field zones of quiet, *Journal of Sound and Vibration* 172 (1993) 605–627.
[8] S.J. Garcia-Bonito, S.J. Elliott, C.C. Boucher, Generation of zones of quiet using a virtual microphone arrangement, *Journal of the Acoustical Society of America* 101 (1997) 3498–3516.
[9] L. Beranek, I.L. Ver, *Noise and Vibration Control Engineering, Principles and Applications*, Wiley/Interscience, New York, 1992.
[10] T. Van Den Dool, N. Doelman, S. Hausler, H. Baier, Broadband MIMO in an Ariane fairing model. *Proceedings of the Active '97*, Budapest, Hungary, 1997, pp. 21–23.
[11] H. Nagamatsu, S. Ise, K. Shikano, Numerical study of active barrier based on the boundary surface control principle, *Proceedings of the ACTIVE '99*, Fort Lauderdale, USA, 1999.
[12] A. Roure, Active noise control of a moving source, *Proceedings of the ACTIVE 2002*, July 15–17, ISVR, Southampton, UK, 2002.
[13] A. Roure, P. Herzog, C. Pinhède, Active barrier for airport noise, *Proceedings of the InterNoise 2006*, Honolulu, 3–5 December 2006.
[14] D.C. Montgomery, G.C. Runger, *Applied Statistics and Probability for Engineers*, Wiley, New York, 2003.
[15] J.B. Allen, D. Berkley, Image method for efficiently simulating small-room acoustics, *Journal of Acoustic Society of America* 65 (4) (1979) 943–950.
[16] H.V. Fuchs, X. Zha, M. Pommerer, Qualifying freefield and reverberation rooms for frequencies below 100 Hz, *Applied Acoustics* 59 (2000) 303–322.
[17] E. De Geest, R. Garcea, Simulation of room transmission functions using a triangular beamtracing computer model, *IEEE ASSP Workshop on Applications of Signal Processing to Audio and Acoustics*, 1995, pp. 253–256.
[18] E.B. Viveiros, B.M. Gibbsb, An image model for predicting the field performance of acoustic louvres from impulse measurements, *Applied Acoustics* 64 (2003) 713–730.
[19] S.J. Elliott, P. Joseph, A.J. Bullmore, P.A. Nelson, Active cancellation at a point in a pure tone diffuse sound field, *Journal of Sound and Vibration* 120 (1988) 183–189.
[20] S. Elliott, Signal Processing for Active Control, Academic Press, New York, p. 219.